Journal of Theoretical Biology 363 (2014) 74–79

Contents lists available at ScienceDirect

Journal of Theoretical Biology

journal homepage: www.elsevier.com/locate/yjtbi

Modelling spatial oscillations in soil borehole bacteria

M.J. McGuinness [a,*], L.B. Cribbin [b], H.F. Winstanley [b], A.C. Fowler [b,c]

[a] School of Mathematics, Statistics and Operations Research, Victoria University of Wellington, New Zealand
[b] MACSI, University of Limerick, Limerick, Ireland
[c] OCIAM, University of Oxford, Oxford, UK

HIGHLIGHTS

- A simple mathematical model.
- Spatial oscillations in groundwater contaminants.
- Microbial competition between fermenters and respiring heterotrophs plays the key role.
- Self-sustained temporal oscillations plus spatial diffusion can give travelling waves.

ARTICLE INFO

Article history:
Received 28 February 2014
Received in revised form
15 July 2014
Accepted 12 August 2014
Available online 21 August 2014

Keywords:
Groundwater contamination
Spatial diffusion
Microbial competition
Travelling waves

ABSTRACT

Spatial oscillations in groundwater contaminant concentrations can be successfully explained by consideration of a competitive microbial community in conditions of poor nutrient supply, in which the effects of spatial diffusion of the nutrient sources are included. In previous work we showed that the microbial competition itself allowed oscillations to occur, and, in common with other reaction–diffusion systems, the addition of spatial diffusion transforms these temporal oscillations into travelling waves, sometimes chaotic. We therefore suggest that irregular chemical profiles sometimes found in contaminant plume borehole profiles may be a consequence of this competition.

1. Introduction

Groundwater contaminant concentration profiles have been observed to oscillate spatially (Broholm et al., 1998; Jones et al., 1999; Smits et al., 2009). In recent work, Fowler et al. (2014) suggested that one mechanism whereby such oscillatory profiles could occur was through a competitive interaction between respiring heterotrophic and fermentative bacteria. In conditions of limited nutrient supply, self-sustained oscillations in both microbe species and nutrient carbon source can occur in a Continuous Stirred Tank Reactor (CSTR) model, and Fowler et al. (2014) suggest that when this model is studied in a spatially inhomogeneous medium, the effects of diffusion may cause oscillatory waves to occur, corresponding to the spatial oscillations which are actually seen. The purpose of the present paper is to demonstrate that this is true.

An extensively studied site of groundwater contamination is the Rexco site in Mansfield, UK, where the ammoniacal waste liquor from a coal carbonisation plant, which operated from the early 1930s to 1970s (Smits et al., 2009), has penetrated some 18 m into unsaturated sandstone, forming a contaminant plume of about 25 m depth. In the course of a large field investigation (Broholm et al., 1998; Jones et al., 1999), groundwater and soil samples were taken from a series of boreholes and the minerals in the aquifer were characterised. The results from borehole BH102 (data collected May 2003) are shown in Fig. 1. Data for each contaminant was recorded along 25 cm intervals beginning 18 m underground at the top of the saturated zone, so that we can see a vertical section through the contaminant plume. The interpretation of data such as these follows standard explanations of redox zonation by sequential depletion of terminal electron acceptors (TEAs) (e.g. Chapelle, 2001). The most striking feature of the data is the nitrate spike at 19 m depth, suggestive of coupled nitrification–denitrification, presumably at the lower margin of the oxic zone, though oxygen data are not available. The steady decrease of nitrate from 19 m to 22.5 m indicates denitrification in the absence of oxygen, with a depletion at 22.75 m in a sharp front. The dominant TEA process in this region is not evident from the data, but dissimilatory iron reduction or sulphate reduction are plausible candidates. Our interest is in the zone below this front (from 23 m depth), where concentrations of the electron donors' organic carbon and ammonium

* Corresponding author: School of Mathematics, Statistics and Operations Research, Victoria University of Wellington, New Zealand. Tel.: +64 4 463 5059.
E-mail address: Mark.McGuinness@vuw.ac.nz (M.J. McGuinness).

http://dx.doi.org/10.1016/j.jtbi.2014.08.017
0022-5193/

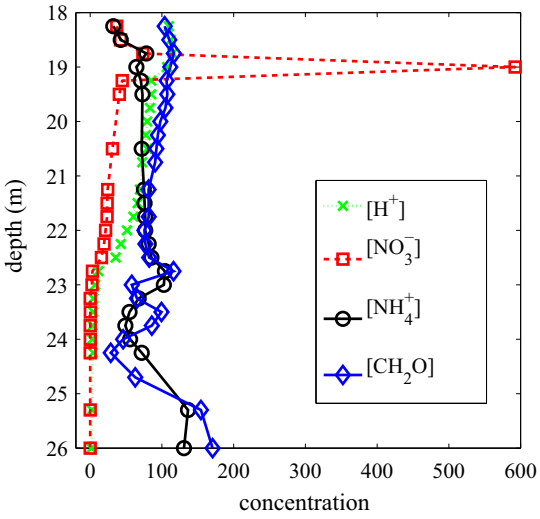

Fig. 1. The data from the Rexco site, borehole 102, May 2003, showing concentrations of NH_4^+ (mg l^{-1}), NO_3^- (mg l^{-1}), H^+ (nmol l^{-1}) and CH_2O (10^{-5} mol l^{-1}). Note that the zero concentration is offset from the left hand axis, and both H^+ and NO_3^- go to zero at a reaction front at depth 22.75 m. Oscillations in concentration profiles are observed from 22.5 m. The data was kindly provided by David Lerner and Arne Hüttmann at the Groundwater Protection and Restoration Group, University of Sheffield.

appear to show out-of-phase spatial oscillations. While only a single period of these oscillations is visible, the important feature is the coherence of the data points within this period; the signal does not appear noisy. Other borehole profiles from the same site also show similar coherent oscillations (Smits et al., 2009). Although oscillations in chemical reactions can occur, for example in the Belousov–Zhabotinskii reaction (e.g., Murray, 2002), we have sought vainly in models of nitrification for processes which might oscillate. Instead, we suggested (Fowler et al., 2014) that the cause of spatial oscillations might lie in competition between microbial populations. While microbial competition is commonly thought of as providing for competitive exclusion (Smith and Waltman, 1995), we showed (Fowler et al., 2014) that in a simple model of microbial competition oscillations could occur.

We wish to emphasise that while our interest in spatial oscillations is motivated by Fig. 1, our concern is not to explain that particular data set, but simply to ask the question whether realistic mathematical models of microbial growth are consistent with such oscillations. The model described in the following section should be divorced from any direct connection with Fig. 1.

The model system which we studied earlier represented a fairly general system in which two competing microbial populations used two different carbon sources, provided typically by hydrolysis from an organic carbon feed. A population of heterotrophs could utilise either source, but preferred the simpler, broken down carbon, which itself was provided by the action of fermenters on the complex source. The resulting activator–inhibitor system led to pronounced oscillations in conditions of relative starvation.

In this short note, we show that the same model kinetics, when incorporated in a spatial domain with the effects of spatial diffusion added, allow spatial oscillations to occur, with a wavelength comparable to that which is seen in Fig. 1, although we emphasise again that a direct application is not intended.

2. Activation-inhibition system

2.1. The model

The interactions between respiring heterotrophic bacteria (H) and fermentative bacteria (F), consuming complex (C_n) and simple (C_1) organic carbon are given by the model (Fowler et al., 2014)

$$\frac{\partial H}{\partial t}=\frac{r_nC_nH}{C_n+K_n}+\frac{r_1C_1H}{C_1+K_1}-d_HH,$$
$$\frac{\partial F}{\partial t}=\frac{r_FC_nF}{C_n+K_F}-d_FF,$$
$$\frac{\partial C_n}{\partial t}=-\frac{r_FC_nF}{Y_{Fn}(C_n+K_F)}-\frac{r_nC_nH}{Y_n(C_n+K_n)}+S+D\frac{\partial^2C_n}{\partial z^2},$$
$$\frac{\partial C_1}{\partial t}=\frac{r_FC_nF}{Y_{F1}(C_n+K_F)}-\frac{r_1C_1H}{Y_1(C_1+K_1)}+D\frac{\partial^2C_1}{\partial z^2}, \quad (2.1)$$

which differs from our earlier model by the inclusion of diffusion terms for the soil carbon concentrations in a one-dimensional spatial domain $-\infty<z<\infty$.

Diffusive transport is assumed here because we are concerned with the vertical structure of the profile. In fact, transport in groundwater plumes is essentially by horizontal advection, and is measured by the size of the (reduced) Péclet number, which has a typical value somewhat larger than one.[1] However, such advection simply causes the vertical diffusive term to be relative to a uniformly advected horizontal spatial coordinate, with respect to which (2.1) provides the appropriate model.

Units for H, F, C_n, and C_1 are $mg_{COD}\,l^{-1}$. Fermenters activate respiring heterotrophs as they break down complex carbon and produce simple organic carbon. The respiring heterotrophic bacteria that consume the complex organic carbon inhibit the fermenters. S denotes the constant source of complex organic carbon and r_i denotes reaction uptake rates. We have used simple Monod uptake terms with maximal uptake rates r_i, half-saturation constants K_i, yield coefficients Y_i, and linear death rates with coefficients d_i, for the bacteria. We have ignored an additional source term for complex carbon released upon death by organic material, involving a conversion ratio ζ, which is noted in Fowler et al. (2014) can lead to chaotic oscillations if $\zeta\neq0$.

Typically, organic carbon would be supplied through advection from upstream, diffusion from the plume centre, or by hydrolysis. The latter would provide a source term in the equation, and following Fowler et al. (2014), we take this source S to be constant.

2.2. Non-dimensionalisation

We non-dimensionalise the equations in the same way as Fowler et al. (2014), additionally choosing an appropriate length scale:

$$H=\frac{S}{d_H}h,\quad F=\frac{S}{d_F}f,\quad C_1=\frac{K_1d_H}{r_1}c,\quad C_n=\frac{K_Fd_F}{r_F}s,$$
$$t\sim t_0=\sqrt{\frac{K_n}{r_FS}},\quad z\sim l=\sqrt{Dt_0}. \quad (2.2)$$

Parameter values are listed in Table 1; these are as given by Fowler et al. (2014), with the additional choice of a diffusion coefficient D of $\sim10^{-9}$ $m^2\,s^{-1}$. Most of the parameter values are taken from Langergraber et al. (2009).

The resulting dimensionless model is given by

$$\varepsilon\lambda h_t=\frac{\delta hs}{1+\gamma s}+\frac{hc}{1+\alpha c}-h,$$
$$\varepsilon f_t=\frac{sf}{1+\beta s}-f,$$
$$s_t=\varepsilon\left[\sigma-\frac{sf}{Y_{Fn}(1+\beta s)}-\frac{\delta hs}{Y_n(1+\gamma s)}\right]+s_{zz},$$

[1] A typical example is for a horizontal flow of $U=10$ m year^{-1}, over a horizontal distance $L\sim1$ km and vertical extent $h\sim10$ m; if the transverse dispersion coefficient is $D\sim10^{-9}$ $m^2\,s^{-1}$, then the reduced Péclet number is $Pe=Uh^2/LD\sim30$.

$$c_t = \varepsilon\mu\left[\frac{sf}{Y_{F1}(1+\beta s)} - \frac{hc}{Y_1(1+\alpha c)}\right] + c_{zz}, \tag{2.3}$$

where the dimensionless parameters are defined by

$$\alpha = \frac{d_H}{r_1}, \quad \beta = \frac{d_F}{r_F}, \quad \gamma = \frac{K_F d_F}{K_n r_F}, \quad \delta = \frac{r_n K_F d_F}{r_F K_n d_H},$$

$$\varepsilon = \frac{1}{d_F t_0}, \quad \lambda = \frac{d_F}{d_H}, \quad \mu = \frac{r_1 K_F d_F}{r_F K_1 d_H}, \quad \sigma = 1. \tag{2.4}$$

Typical parameter values are listed in Table 2.

If the diffusion terms are neglected, these equations have solutions consisting of self-sustained oscillations. An example is shown in Fig. 2. The profile of s is similar to a sawtooth oscillation. The bacteria profiles are spiky in nature and become more spiky with small values of ε, which represents starvation in the system.

Table 1
Values of the constants as estimated by Fowler et al. (2014).

Symbol	Typical value
d_F	0.02 d^{-1}
d_H	0.2 d^{-1}
D	10^{-9} m^2 s^{-1}
K_n	2 mg_{COD} l^{-1}
K_1	4 mg_{COD} l^{-1}
K_F	28 mg_{COD} l^{-1}
l	0.25 m
r_n	2.4 d^{-1}
r_1	2.4 d^{-1}
r_F	1.5 d^{-1}
S	0.37×10^{-4} mg_{COD} l^{-1} d^{-1}
t_0	0.71×10^3 d
Y_n	0.63
Y_1	0.63
Y_{Fn}	0.053
$Y_{F\,1}$	18

Table 2
Typical values of the dimensionless parameters.

Parameter	Typical value
α	0.08
β	0.013
γ	0.18
δ	2.2
ε	0.07
λ	0.1
μ	1.1

The issue of boundary and initial conditions requires some consideration. On an infinite domain, we seek to prescribe s and c at $z = \pm\infty$. Our thesis is predicated on the idea that a pre-existing quiescent state is activated by the arrival of a plume (at, we suppose, $z=0$), and then initiates spontaneous oscillations which propagate outwards from the plume centre.

Since we presume that the parameters are such that oscillations occur, the only sensible boundary conditions to apply at $\pm\infty$ are those corresponding to the unstable steady state of the system. Defining

$$\delta^* = \frac{\delta}{1-\beta+\gamma}, \tag{2.5}$$

and assuming that

$$\beta < 1, \quad \delta^* < 1, \quad \alpha < \frac{1}{1-\delta^*}, \tag{2.6}$$

then the steady state of the system is

$$s = s^* = \frac{1}{1-\beta}, \quad c = c^* = \frac{1-\delta^*}{1-\alpha+\alpha\delta^*},$$
$$f = f^* = \frac{Y_n Y_{F1} Y_{Fn}(1-\delta^*)}{\delta^* Y_1 Y_{Fn} + (1-\delta^*) Y_n Y_{F1}},$$
$$h = h^* = \frac{Y_1 Y_n Y_{Fn}}{\delta^* Y_1 Y_{Fn} + (1-\delta^*) Y_n Y_{F1}}, \tag{2.7}$$

and suitable boundary conditions are

$$c \to c^*, \quad h \to h^* \quad \text{as } z \to \pm\infty. \tag{2.8}$$

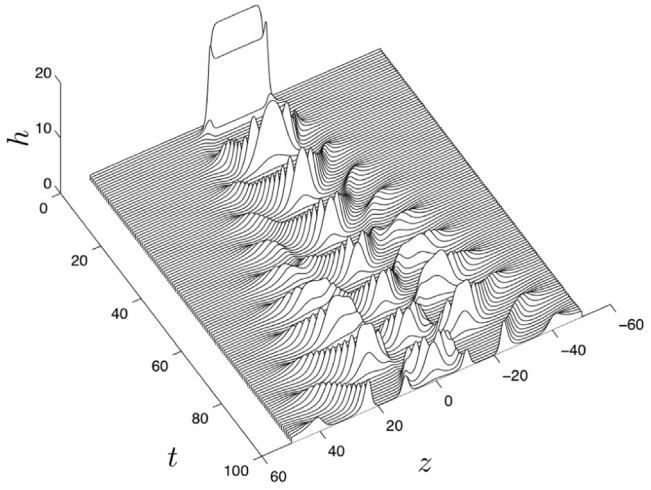

Fig. 3. Waterfall plot of h with parameter values: $\sigma = 1$, $\varepsilon = 0.3$, $\delta = 0.5$, $\mu = \lambda = D = Y_F = Y_n = Y_1 = Y_H = 1$, $\alpha = \beta = \gamma = 0.3$, $\Delta t = 0.5$ and $\Delta z = 0.25$. Initial values are at the unstable steady state, with a superimposed top hat profile for s, as described in (2.9) and (2.10).

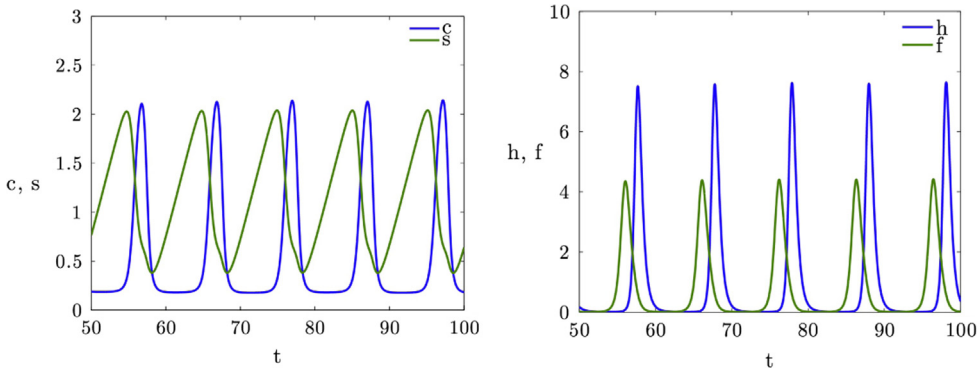

Fig. 2. Solution of (2.3) with the diffusion terms neglected, and the following parameter values: $\varepsilon = 0.3$, $\delta = 0.5$, $\mu = \lambda = Y_F = Y_n = Y_1 = Y_H = 1$, $\alpha = \beta = \gamma = 0.1$.

Initial emplacement of a plume is then represented by taking initial conditions

$$f = f^*, \quad h = h^*, \quad c = c^* \quad \text{at } t = 0, \tag{2.9}$$

together with a top hat initial profile for s

$$s = \begin{cases} s_0 & |z| < z_0 \\ s^* & |z| > z_0 \end{cases} \quad \text{at} \quad t = 0, \tag{2.10}$$

and we would typically take $z_0 = O(1)$, $s_0 \gg 1$.

2.3. Results

The model in (2.3) was solved by the method of lines in the positive half of the domain. The result was then reflected across the z-axis producing the symmetrical solution.

Figs. 3–5 show the results of a numerical solution of the equations using the initial and boundary conditions given in (2.9) and (2.10), respectively.

Fig. 3 shows the evolution of the heterotrophic bacteria. The initial emplacement of an enrichment of s causes a rapid increase locally in h and an equally rapid decline, similar to the spiky oscillations in Fig. 2. However, just as in the temporal oscillations, there continue to be subsequent spikes, but the effect of diffusion is to cause a spreading of the oscillatory behaviour, so that at any particular time, h exhibits spatial oscillations. A sequence of snapshots of h and s at different times is shown in Fig. 4.

Fig. 5 shows the corresponding waterfall plot for the complex carbon s. The behaviour is similar, although as we expect the oscillations are less abrupt. An interesting feature, seen in both Figs. 3 and 5, is that while there is net propagation of the profiles outwards, the oscillatory peaks are actually formed by propagation of growing waves inwards from the far field. It may be noted that although the waterfall plots have an appearance that is suggestive of a large-scale order, due to the temporal behaviour being dominated by the stable limit cycle that obtains for a single set of populations, the individual snapshots are suggestive of more irregular spatial oscillations. Details of whether in fact the waves

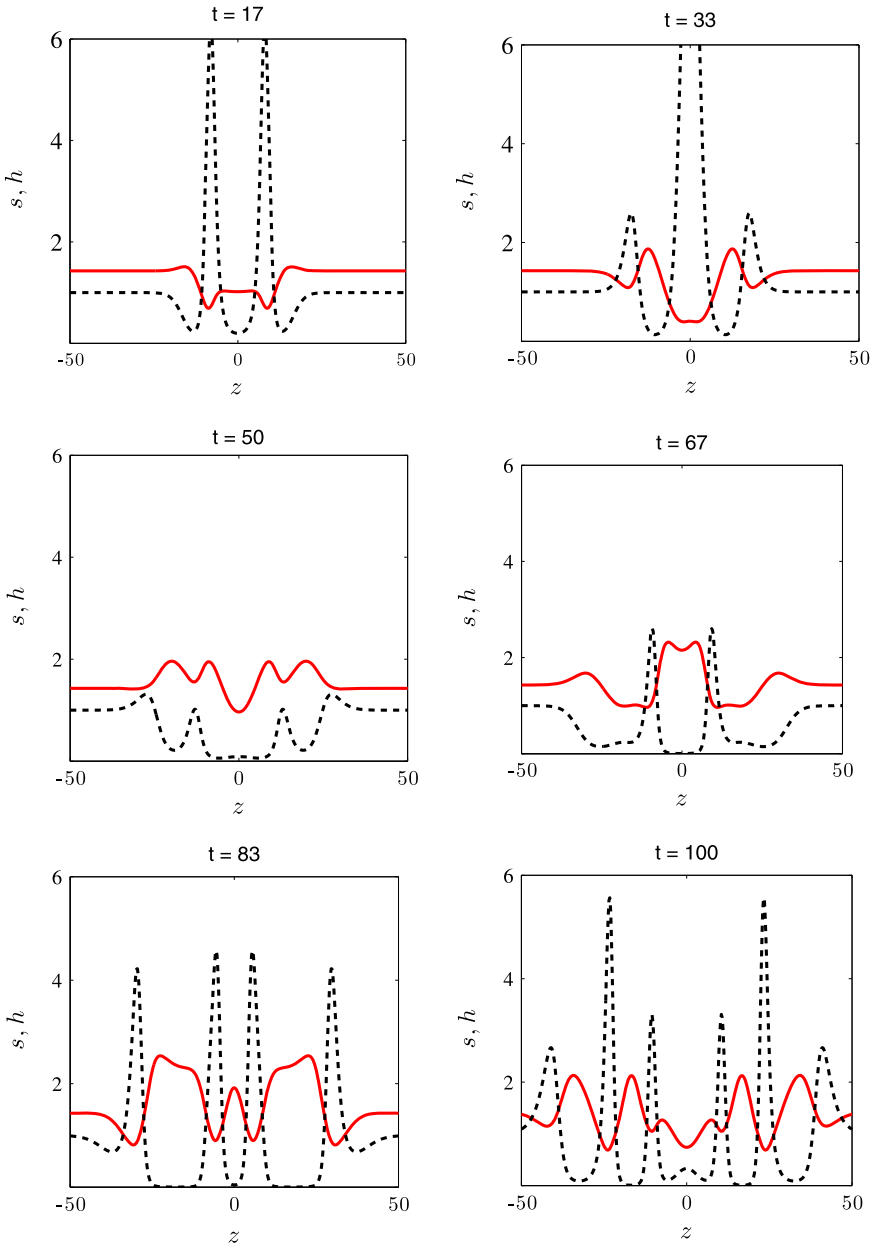

Fig. 4. A sequence of snapshots at the indicated dimensionless times of the evolving h (dashed lines) and s (solid lines) values. Parameter values are as in Fig. 3.

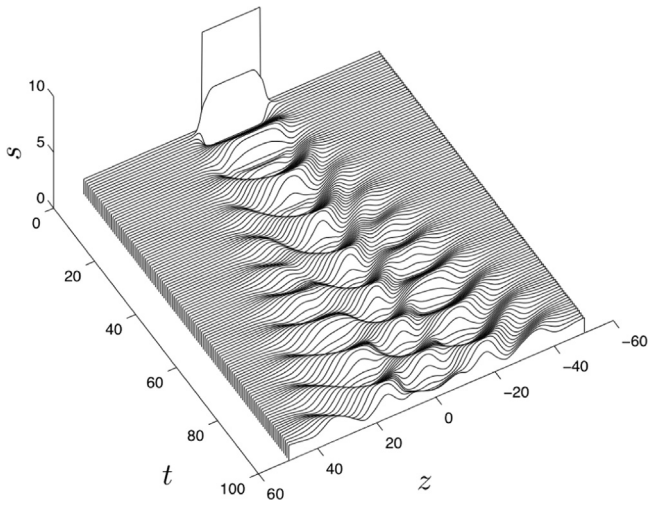

Fig. 5. Waterfall profile for s, parameters as in Fig. 3.

are a manifestation of chaotic or quasi-periodic behaviour are of interest, but will be pursued elsewhere.

While the model system we have studied is motivated by the apparent oscillations seen in Fig. 1, we emphasise again that it is *not* designed to simulate the actual data of that figure, rather we are simply endeavouring to answer the question as to whether realistic microbiological population models will allow the occurrence of such oscillations. Despite the fact that our aim is not to simulate Fig. 1, one feature of that figure bears further scrutiny, and that is the apparent wavelength of the oscillation. If our heterotroph-fermenter model provided vastly different wavelengths to those in the figure, it would provide a genuine cause for concern; therefore it is of interest to compare these wavelengths. The spatial wavelength of the oscillations observed in the snapshots of numerical solutions are of the order of 5–10 dimensionless units, which corresponds, with a length scale $l=0.25$ m (see Table 1), to a dimensional wavelength of 1.25–2.5 m. This is roughly comparable to the 1 m wavelength suggested by the CH_2O data in Fig. 1, and to the 2 m wavelength suggested by the NH_4 data, and at least indicates a consistency in the model. Considering the definition of l in (2.2), the principal uncertainty in the wavelength lies in the constituents of the time scale t_0, which in particular involves the uncertain supply term S; however, note from (2.4) that we can also define

$$l=\sqrt{\frac{D}{\varepsilon d_F}}, \tag{2.11}$$

so that we expect the wavelength to be associated primarily with the value of ε, and more particularly with the period of the oscillations which occur in the spatially homogeneous case. This dependence has been studied by Fowler (2014), who shows that the dimensionless period of the oscillation is of order $1/\varepsilon^2$, but also that the bacterial populations reach minima of $O[\exp\{-O(1/\varepsilon^2)\}]$. Such small minima suggest effective extinction of the bacteria, and replacement in the community by competitors. Roughly speaking, oscillations occur for $\varepsilon\lesssim 1$ but quickly become untenable as ε is reduced. The suggestion is then that the period and consequent wavelength of the oscillations will be relatively robust over the fairly narrow range where starvation occurs. The word starvation is used here as a proxy for resource limitation. And, of course, starvation is precisely the mechanism in a plume whereby the successive TEAs are brought into play. The interesting question of the interaction between the depletion of TEAs and the formation of spatial oscillations awaits further study.

3. Conclusions

A basic principle of reaction–diffusion theory is that when a spatially homogeneous reacting system exhibits limit cycle oscillations, then when placed in a medium where the reactants can diffuse, travelling waves result (Fowler, 2011, pp. 41 ff.; Murray, 2002; Kopell and Howard, 1973; Keener, 1980), and this principle has been used effectively to explain periodic waves in the Belousov–Zhabotinskii reaction, wave propagation in nerve cells, and also chaotic waves in predator–prey systems quite similar to the set-up considered here (Sherratt et al., 1995).

Thus, motivated by this guiding principle, and also by the admittedly limited but nevertheless compelling evidence of plots such as that in Fig. 1, which seem to imply spatial oscillations in soil chemistry profiles, we began the search for an oscillatory reactive mechanism. We have yet to discover a soil chemical reaction set which oscillates, but we did find that by shifting the focus to the interactions between microbes, we could identify a simple competitive microbial model which does oscillate (and does so robustly). Our presumption then was that with the inclusion of suitable diffusion terms for the mobile constituents (i.e.,the nutrients), spatial oscillations in the form of travelling waves would occur, and indeed this is what we have found: this is the principal conclusion of the present paper.

In our interpretation of Fig. 4, the z-axis would represent a vertical borehole profile, with $z=0$ representing the centre of a groundwater plume, and (analogously to Fig. 1) depth increasing with z. One conclusion of interest is that although the reaction kinetics are periodic, the outward propagating waves appear irregular; the same thing was found by Sherratt et al. (1995). Another, which we are hesitant to emphasise, is that if one compares Figs. 4 to 1, the second panel at $t=33$, dimensionally corresponding to 66 years, shows a waveform in s over a distance $z\sim 20$ from the centre of the plume, corresponding to 5 m, which is surprisingly similar to the ammonium profile in Fig. 1. We do not read explanation into this similarity, but the confluence of time and space scale is reassuring even if not suggestive (recall that the plant operated from the 1930s until 1970, while 66 years before the borehole sampling date of 2003 is 1937).

Two further features of the results are of note. At a reaction front, such as that exhibited at 22.75 m depth in Fig. 1, we would expect the reactant concentrations to go to zero (Hagan et al., 1985), but the oscillating CH_2O and NH_4^+ profiles do not show this. Neither in fact does the ammonium go to zero at the higher level nitrate spike at 19 m, which we might expect on the basis of the simple nitrification reaction

$$NH_4^+ + 2O_2 \rightarrow NO_3^- + H_2O + 2H^+. \tag{2.12}$$

These observations are consistent with our results, in which spatial oscillations propagate into a background field of non-zero ambient concentration.

A second feature of interest is that although the purely temporal oscillations are periodic, the resulting spatial travelling waves are less regular. The waterfall plots of s and h are suggestive of quasi-periodic motion in space and time, but this is not obvious in the snapshots of the spatial concentrations, which at face value indicate a more noisy profile, as also found by Sherratt et al. (1995). We therefore suggest that even irregular oscillatory soil chemical profiles may reflect an underlying mechanism of oscillation in microbial populations, possibly associated with depletion of the relevant terminal electron acceptor, and are not simply the result of noise in field measurement.

Acknowledgements

A.C.F. acknowledges the support of the Mathematics Applications Consortium for Science and Industry (www.macsi.ul.ie) funded by the Science Foundation Ireland Grant 12/IA/1683. This publication has emanated from research conducted with the financial support of Science Foundation Ireland under Grant no. 09/IN.1/I2645.

References

Broholm, M.M., Jones, I., Torstensson, D., Arvin, E., 1998. Groundwater contamination from a coal carbonization plant. In: Lerner, D.N., Walton, N.R.G. (Eds.), Contaminated land and groundwater, future directions. Geol. Soc. Lond. Eng. Geol. Special Publ. 14(1), 159–165.

Chapelle, F.H., 2001. Ground-Water Microbiology and Geochemistry. John Wiley, New York.

Fowler, A.C., 2011. Mathematical Geoscience. Springer-Verlag, London.

Fowler, A.C., 2014. Starvation kinetics of oscillating microbial populations. Math. Proc. R. Ir. Acad. (in press).

Fowler, A.C., Winstanley, H.F., McGuinness, M.J., Cribbin, L.B., 2014. Oscillations in soil bacterial redox reactions. J. Theoret. Biol. 342, 33–38.

Hagan, P.S., Polizzotti, R.S., Luckman, G., 1985. Internal oxidation of binary alloys. SIAM J. Appl. Math. 45, 956–971.

Kopell, N., Howard, L.N., 1973. Plane-wave solutions to reaction-diffusion equations.

Keenes, J.P., 1980. Waves in excitable media. SIAM J. Appl. Math. 39, 528–548.

Jones, I., Lerner, D.N., Baines, O.P., 1999. Multiport sock samplers: a lowcost technology for effective multilevel ground water sampling. Ground Water Monit. Remediat. 19 (1), 134–142.

Langergraber, G., Rousseau, D.P.L., Garcia, J., Mena, J., 2009. CWM1: a general model to describe biokinetic processes in subsurface flow constructed wetlands. Water Sci. Technol. 59, 1,687–1,697.

Murray, J.D., 2002. Mathematical biology (two volumes), Springer-Verlag, Berlin.

Sherratt, J.A., Lewis, M.A., Fowler, A.C., 1995. Ecological chaos in the wake of invasion. Proc. Natl. Acad. Sci. USA 92, 2524–2528.

Smith, H.L., Waltman, P., 1995. The Theory of the Chemostat. CUP, Cambridge.

Smits, T.H.M., Hüttmann, A., Lerner, D.N., Holliger, C., 2009. Detection and quantification of bacteria involved in aerobic and anaerobic ammonium oxidation in an ammonium-contaminated aquifer. Bioremed. J. 13 (1), 41–51.